Empirical Scaling Analysis of Atomising Annular Liquid Sheets

D. Duke*, D. Honnery, J. Soria
Laboratory for Turbulence Research in Aerospace & Combustion
Department of Mechanical & Aerospace Engineering
Monash University, Australia

Abstract

Annular liquid sheets are canonical, unstable multiphase shear flows. Many numerical, theoretical and empirical investigations of such flows have been undertaken, however agreement between studies is limited. This is due in part to the lack of agreed definitions for the gas-liquid momentum scaling and the lack of a canonical geometry, among other factors. Few scaling theories for the periodic driving instability that characterises the atomisation mechanism have yet been proposed which show repeatability between different experimental studies. There have been particularly few investigations into sheet thickness effects, due to the difficulty of manufacturing a test nozzle with a variable thickness. We present a large, parametric, experimental study of a non-swirling annular water sheet exposed to separately metered dual air co-flows over an order of magnitude variation in Reynolds and Weber Numbers. Three sheet thicknesses and a wide range of gas co-flow rates have been considered. We have considered a temporal analysis of the primary interfacial instability using Fourier techniques. From empirical data, a geometry-independent temporal scaling based on a non-dimensional momentum ratio is proposed, which shows good agreement with empirical data on low pressure air-water annular flows over a range of geometries, *Re* & *We*. This scaling is counter-intuitively different from that of the more well-known planar sheet. Through the use of Dynamic Mode Decomposition, the leading Koopman modes of the primary instability provide a spatially resolved reconstruction of the spatial growth rate and amplification profile of the instability. Sheet thickness effects are observed to dominate over all other scaling variables with regard to the amplitude of the instability, within the limits of experimental error. We demonstrate a comparison between the empirically derived complex wavenumber and linear stability analysis. The measured wavenumber approaches the linear solution as we move toward the nozzle. The temporal scaling of annular sheets may follow a predictable scaling, but the spatial scaling behaviour shows a much more complex behaviour dominated by sheet thickness effects due to both non-linearity and non-parallelism.

Introduction

The study of instability in liquid sheets by means of experimentation is limited by two key factors; the need for very high simultaneous spatial and temporal resolution, and the large number of independent variables required to describe the boundary conditions. The need for high resolution is a problem which is being solved in part by modern high-speed high-capacity digital video cameras, however the parametric space problem remains. A liquid sheet issuing into a gaseous environment requires at least 8 independent non-dimensional quantities to describe its behaviour, making a fully crossed, well-resolved parametric analysis unwieldy. Whilst the effects of varying individual variables may be obtained by theoretical analysis [1], a large experimental parametric study has not been achieved to date. The well-established independent non-dimensional quantitites are the Reynolds, Weber, Froude and Ohnesorge Numbers;

$$Re_h = \left(\overline{U}h/\nu\right)_w, \tag{1}$$

$$We_h = \left(\rho\overline{U}^2 h/\sigma\right)_w, \tag{2}$$

$$Fr_h = \overline{U}_w/gh, \tag{3}$$

$$Oh = \sqrt{We}/Re, \tag{4}$$

and the gas-liquid kinematic viscosity and density ratios N and Q respectively. The quantities describing the mean inlet velocities $\overline{U}$ of each flow (for the annular sheet there are three) and the geometry of the nozzle do not have universally agreed definitions due to the suitability of different scalings for different flows. We consider the lengthscale h to be the full thickness of the annular sheet at the nozzle exit.

The optimum choice of non-dimensional scaling for the gas-liquid velocity is also a matter of debate depending on the geometry. The simplest representation is the velocity ratio $VR_j = \overline{U}_j/\overline{U}_w$, for subscript $j = i, o$ being the

*Corresponding author: daniel.duke@monash.edu

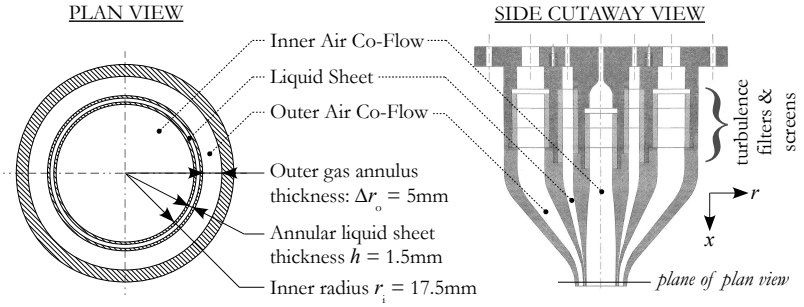

Figure 1: Annular nozzle geometry. A plan view of the nozzle at the exit plane and a cutaway view of the axisymmetric nozzle are shown. The outer gas and liquid sheet annuli have contractions of 4.6:1 and 7.3:1 respectively. The inner gas co-flow has an expansion of 1.3:1. Nozzle diagram reproduced with permission [15].

inner and outer gas phase flows and subscript w indicating the liquid phase. Lozano et al. [2, 3] has proposed geometric and geometrically-independent gas-liquid momentum flux ratios, which we will also consider in the annular regime;

$$MR_{1j} = \left(\rho\overline{U}^2\right)_j / \left(\rho\overline{U}^2\right)_w \equiv Q \cdot VR_j^2, \tag{5}$$

$$MR_{2j} = \left(\rho\overline{U}^2 A\right)_j / \left(\rho\overline{U}^2 A\right)_w \equiv Q \cdot VR_j^2 \cdot \frac{d_j}{h}, \tag{6}$$

where A is the area of the co-flowing gas layer or liquid sheet respectively.

A number of experimental studies have been carried out for aerodynamically driven annular sheets to which we can compare results [4, 5, 6, 7, 8]. Lozano et al. [3] found that a square root thickness Strouhal Number $St = f\sqrt{hd_{gas}}/\Delta U$ collapsed within experimental uncertainty for a plane sheet as a function of MR_2 which is dependent on the geometry. We seek a similar scaling for the annular sheet.

Some attempts have been made to make growth measurements for non-annular geometries [2, 4, 9, 10]. Tammisola et al. [10] have recently shown excellent agreement between linear theory and experiments for the plane sheet, but a similar comparison for the annular sheet has not been done. The non-linearity and non-parallelism in the flow adds additional complication. Recently, we have shown that the complex wavenumber k has been shown to vary as a function of streamwise distance from the nozzle in the annular case [11].

In this paper, we present a parametric study of an empirical annular liquid sheet. Utilising previously published techniques [12, 13, 14] and building on our previously published results [11] we develop a new empirically-derived scaling for the temporal component of the primary shear layer instability. We compare these scaling behaviours against a number of existing studies, to show that a momentum - frequency relationship similar to that of Lozano et al. [3] can be established for the annular case which agrees favourably with over 25 years of empirical data. We also investigate scaling behaviours for the amplification derived from the measured growth rates, showing that the sheet thickness has a dominant effect on the instability amplitude. A direct comparison with linear stability analysis is also shown, which has not been previously reported for this geometry.

Method

The annular liquid sheet nozzle used in this study is shown in Figure 1. An inner core gas flow and outer annular flow surround a thin liquid sheet created by a series of interchangeable, concentric nozzles. The working liquid is water at room temperature, which is supplied by a recirculating pump and reservoir system. The inner and outer gas flows are supplied from an air compressor, and are separately metered. Perforated plates and 1mm^2 turbulence screens before passing through a contraction which aligns the flows parallel to the vertical axis. Hot-wire anemometry of the gas co-flows shows that the air flow is purely axial and is steady [12].

High speed digital imaging of the sheet is performed with a *PCO DIMAX* camera at 7.5kHz, with an exposure time of $10\mu s$. A large pulsed LED array provides back illumination. The outer liquid-gas interface upstream of breakup is imaged at a resolution of 48 pixels/mm (21μm/pixel) - see Figure 2. High-speed, high-definition movies of the flow at a range of conditions can be found online * [12, 13].

*http://youtu.be/XOvk6NumQkw

Figure 2: Sample unfiltered image of spray from annular nozzle. Exposure time is 10μs. Instability properties are measured at the outer sheet surface in the intact upstream region via correlation image velocimetry.

The temporally and spatially resolved normal velocity of the sheet surface $u(x,t)$ is measured from the high-speed images using a digital image correlation method. An error sensitivity analysis of this technique has demonstrated a maximum expected uncertainty in u of $\pm 0.085\overline{U}_w$ at a confidence interval of 99.7%, with a typical mean uncertainty of $\pm 0.030\overline{U}_w$ [12]. Note the non-dimensional velocity u' is scaled by the bulk liquid injection velocity $\overline{U}_w$. The raw time-series velocity data $u'(x,t)$ is not shown here due to space restrictions; typical examples can be found in [11, 12, 13]. A Fourier analysis of the time-series $u'(x_j,t)$ yields the instability spectrum [12]. By taking the spectrum of each time-series for a range of x/h, a continuously evolving spectrum space is extracted, and frequency components are spatially tracked.

The complex wavenumber k is further derived from a spatial Koopman analysis of u', which is calculated using the Dynamic Mode Decomposition (DMD) algorithm of Schmid [16]. A complex, spatially-resolved wavenumber $k(x)$ is derived from the leading (most unstable) DMD eigenvalue by applying a sliding window to the spatial domain [11]. The window width is a key factor in the uncertainty of k, leading to a trade-off between spatial smoothing and instantaneous uncertainty. In this study, a window of $2h$ is applied such that $k(x)$ represents the average linear growth rate within a window of $x \pm h$ and an uncertainty on $k_i(x)$ of typically 10% (maximum 25%). The relatively large uncertainty is mainly due to the sawtooth nature of the surface wave and the trade-off between limiting the window size to obtain a better spatial resolution of $k(x)$ and enlarging the window to reduce the uncertainty [14, 11]. The amplification envelope of the instability is thus calculated via the integral of the growth rate, which we denote the amplification curve $A(x) = \int_0^x k_i(x)dx$.

A partially-crossed parametric study has been undertaken, comprising 3 sets of *We* & *Re* over an order of magnitude variation, 3 sheet thicknesses comprising an approximately 125% variation in the curvature/thickness ratio h', 8 outer gas shear flow rates and 7 inner gas shear flow rates. Conditions are listed in Table 1.

Results & Discussion

At all studied conditions, we find a peak frequency which is independent of x/h, which agrees with previous results [12]. The power spectral density grows to a peak in the free shear layer as the quasi-sinusoidal instability amplifies, and then decays but remains prominent once the sheet breaks up. The frequency, which originates at the nozzle exit due to the mixed Kelvin-Helmholtz Rayleigh-Taylor instability in the free shear layer, dominates the entirety of the resulting spray, such that ligaments and droplets are formed in waves or bunches, resulting in periodic (not continuous) formation of droplet clusters. The empirical scaling behaviour of the peak frequency reveals a quadratic relationship with the shear velocity. Figure 3a demonstrates the parametric dependence of *St* on $\Delta\overline{U}_{i,o}$. We are able to fit a quadratic least-squares function to this data of the form

$$St \approx a_0 + a_1\Delta\overline{U}_i + a_2\Delta\overline{U}_i^2 + a_3\Delta\overline{U}_o + a_4\Delta\overline{U}_o^2 + a_5\Delta\overline{U}_i\Delta\overline{U}_o, \tag{7}$$

with excellent agreement ($R^2 = 0.99$). The uncertainty in *St* is based on the half-width of the Fourier peak, as the time series is not distinctly sinusoidal and the instantaneous frequency may vary around the mean. The values

Independent Variable	**Values**
sheet thickness h, mm	0.67, 1.0, 1.5
curvature/thickness ratio h'	13, 19, 29
Re	500, 2400, 4200
U_w, ms^{-1}	0.55, 2.44, 4.44
$\Delta\overline{U}_i, ms^{-1}$	0, 3.30, 6.60, 9.50, 12.87, 16.31, 20.00 (at $\Delta\overline{U}_o = 1.85,\ 18.83,\ 32.00\ ms^{-1}$)
$\Delta\overline{U}_o, ms^{-1}$	1.85, 5.73, 10.12, 14.47, 18.83, 23.21, 27.53, 32.00 (at $\Delta\overline{U}_u = 0,\ 9.50,\ 20.00\ ms^{-1}$)
Q	1.2×10^{-3} (water and air at 23°C)
N	15 (water and air at 23°C)
Derived Quantities	**Values**
We	2.5, 3.6, 5.3, 57, 83, 122, 173, 253, 430
Oh	3.05×10^{-3} 3.73×10^{-3} 4.56×10^{-3}
Fr	21, 31, 47, 405, 607, 906, 1340, 2015, 3000
MR_i	0 – 5.06 (63 discrete values)
MR_o	0 – 11.22 (72 discrete values)

Table 1: Experimental conditions for parametric study. The independent variables are defined, and the quantities derived from combinations of these (Such as *We* and *MR*) are given below.

of a_n vary depending on *Re* & *We* as expect, but also vary with sheet thickness h due to a combination of non-linearity and non-parallelism. We therefore seek an alternative global scaling which may be independent of these parameters.

Since the non-dimensional representations for the shear velocity ($MR_{1,2}$) are proportional to the square of $\Delta\overline{U}_{i,o}$, we hypothesise an approximately linear relationship between *MR* and a non-dimensional frequency *St*. As the inner and outer gas flows both show a similar relationship with *St*, it may be further possible to combine $MR_{i,o}$ into a Total Momentum Ratio, which represents the sum total shearing energy at both interfaces;

$$TMR_{1,2} = MR_{1,2i} + MR_{1,2o}. \tag{8}$$

If the annular sheet scales similarly to the plane sheet, we expect to see a collapse with TMR_2 and *St* based on $\sqrt{h}$ and ΔU. However, this is not the case. Instead, we find that for the annular geometry, the collapse occurs for the *geometry indepdenent* TMR_1 and $St = fh/U_w$, which is based on the full sheet thickness and the absolute liquid velocity[†]. This is a surprising result. The dependence of *St* and *TMR* is shown in Figure 3b for the full database (all *Re*, *We* & h values). At high *TMR*, *St* follows a strongly linear trend. This trend appears independent of h. Both inner and outer gas flows are varying in Fig. 3b, which suggests that *St* & *TMR* accounts for the effects of both inner and outer gas flows. The observed behaviour is consistent over an order of magnitude variation in *Re* and two orders of magnitude variation in *We*.

For $TMR < 1$, some outliers from the predicted trend are observed. Figure 3b shows that these outliers are explained by cases in which the flow is not in a regime of continuous atomisation. In this case, the atomisation quality is based on a qualitative observation of droplet formation from the high speed images. 'No atomisation' corresponds to cases where an instability may appear but damps out and the flow breaks up via only capillary instability of the liquid column, in which little to no droplet formation results. 'Marginal atomisation' corresponds to cases where some instabilities produce atomisation of the flow, and some do not. 'Complete atomisation' is a regime in which each cycle of the instability mechanism produces droplets. It is observed that complete atomisation always occurs for $TMR \geq 1$.

Although we hypothesise a linear relationship, a linear fit to the frequency data of Figure 3b returns a relatively poor quality of fit ($R^2 \approx 0.8$). If the linear fit is modified by the addition of a logarithmic term, a far superior least-squares fit is obtained. Our modified fitting function thus takes the form

$$St \approx \alpha_0 + \alpha_1(TMR) + \alpha_2 TMR \log_e(TMR). \tag{9}$$

[†] From herein we use *TMR* in place of TMR_1

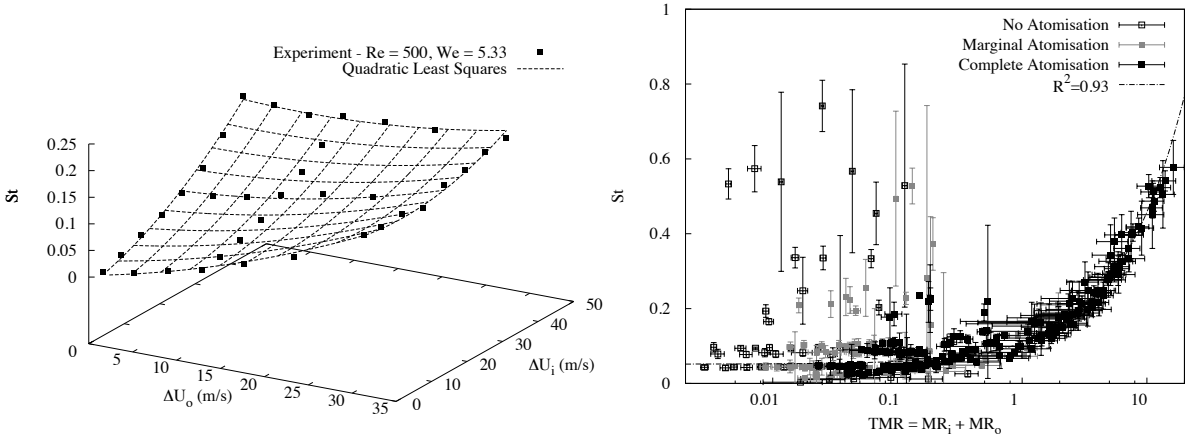

(a) Strouhal Number of dominant instability vs. $\Delta\overline{U}_{i,o}$ at $Re = 500$, $We = 5.33$, $h' = 13$. A least-squares parametric polynomial fit demonstrates the quadratic dependence of *St* on $\Delta\overline{U}_{i,o}$. The quality of the fit is $R^2 = 0.99$.

(b) Dominant frequency of instability, as a function of total momentum ratio. Data points are categorised by the quality of atomisation. Error bars in *TMR* represents uncertainty, error bars in *St* represent the Fourier peak half-width.

Figure 3: Frequency data for annular sheet, obtained via Fourier analysis.

The constants α are calculated via an iterative, non-linear least squares Marquardt - Levenburg algorithm. The resulting values are given in Table 2, with $R^2 = 0.93$ for all data, and the fitting function is shown for the full population in Figure 3b. No selective removal of outliers has been performed.

The global scaling function of Eqn. 9 is compared to frequency measurements for other annular liquid sheets in Figure 4a and other non-annular geometries in Figure 4b. A number of other experiments exhibit a similar scaling behaviour, despite the fact that these experiments all exhibit arbitrarily varying geometries and different *Re* and *We*. The collapse occurs once *TMR* is used as the gas-liquid momentum scaling. It should be noted that the frequency of the DNS of Siamas et al. [17] is based on centerline velocity rather than interfacial velocity. We observe that the plane sheet data in Fig 4b does not collapse as well for higher *TMR*, but rather follows the scaling already outlined by Lozano et al. [3]. This suggests that annular sheets follow a different scaling behaviour to plane sheets, and the question then arises as to what radius of curvature may lead to the transition between one scaling regime and the other. This is a matter for future investigation.

Through the use of Koopman analysis via Dynamic Mode Decomposition (DMD), the spatially resolved complex wavenumber $k(x)$ may also be determined. From this, the overall amplification curve $A(x)$ may be calculated. Figure 5 shows profiles of $A(x)$ for all experimental conditions. The sheet thickness is observed to have a strong effect on the amplification magnitude, and also causes some stretching in x/h, which suggests that the appropriate non-dimensional length scale is not h, but some modified length scale. We hypothesise that the sheet thickness may act as a global scaling factor on the amplification profile. We therefore define a rescaled amplification and length scale (denoted by asterisk) which are independent of the sheet thickness;

$$A^*(x) = A(x) \cdot h^{\beta_0}, \text{ and} \tag{10}$$

$$x^* = x \cdot h^{\beta_1}. \tag{11}$$

The non-linear least-squares calculation yields $\beta_0 \approx 4/3$ and $\beta_1 \approx -3/5$ as the rescaling factors. The sheet thickness has a super-linear effect on the amplification profile and a sub-linear effect on the stretching of the instability in x, such that increasing thickness causes an increasing in amplification and a contraction in x. We acknowledge that determination of $\beta_{0,1}$ is limited by the uncertainty in the individual amplification profiles, which is relatively large. Given approximately 30,000 ensemble-averages at each condition and over all 428 experimental conditions we are able to fit the same $\beta_{0,1}$, so the size of the database compensates somewhat for the high instantaneous uncertainty in the DMD. As a result, uncertainty in β is estimated at $\pm 2\%$.

We now seek a comparison with the growth rate $k(x)$ mesaured by DMD with predictions of this quantity from linear stability analysis. Figure 6 shows a comparison between experiments and the spatial linear solution plane of [1]. Lin's calculation is a contour map of spatial solutions to the dispersion relationship at various frequencies, as indicated by the dashed lines. The solution plane predicts a saddle point (denoted $\times$) which represents the most unstable frequency. The function $k(x)$ from our experiments may be represented as a 'streamline', indicating the

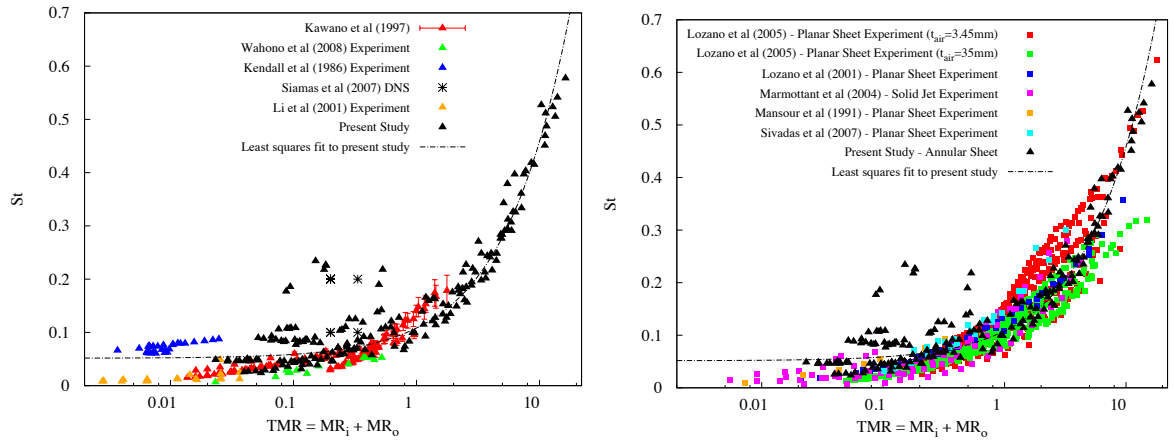

(a) Studies of annular sheets, after [15], [17], [6], [4] & [8]. Error bars of [4] represent half-width of the Fourier peak. Reasonable agreement is observed.

(b) Non-annular geometries, after [18], [3],[9], [2] & [19]. Somewhat reduced collapse is observed.

Figure 4: Dominant frequency of instability, non-dimensionalised as Strouhal Number, as a function of gas-liquid total momentum ratio. Comparsion is shown between the present study (non-atomising cases excluded) and a range of studies for annular and non-annular geometries.

Coefficient	Value	Asymptotic Standard Error	95% Confidence Interval
α_0	5.152×10^{-2}	4.60×10^{-3}	9.04×10^{-3}
α_1	5.665×10^{-2}	6.12×10^{-3}	1.20×10^{-2}
α_2	-6.949×10^{-3}	2.97×10^{-3}	5.84×10^{-3}

Table 2: Table of coefficients for the proposed global Strouhal Number - Momentum relationship of Eqn. 9. Asymptotic standard errors based on the Marquardt - Levenburg non-linear least squares algorithm and confidence intervals at 95% from t-distribution are given.

continuously varying path of $k(x)$ through the complex plane as x increases. It should be noted that we use the term 'streamline' in an abstract sense, as we are not following a physical parcel of fluid but rather a property of the time-mean instability mechanism through the complex plane of k.

We observe reasonable agreement between the experiment (solid vectors) and linear prediction in the near-field. The experimental measurement begins near the predicted saddle point and rapidly diverges toward reducing wavenumber and reducing instantaneous growth rate. The measured values of k depart from the solution domain of [1] within one sheet thickness from the nozzle exit. In some cases, the departure of the measured k from the domain is so rapid that the streamline cannot be accurately tracked all the way to the edges of the domain as the changes in k become too rapid for our spatial resolution of $21\mu m$ per pixel. As a result, some streamlines in Fig. 6 end before leaving the graph. Deviations from the linear solution appear to already be present in the solution at the near-field measurement points several tens of μm from the nozzle. These may be due to a combination of non-linear growth and also non-parallelism in the real flow.

The dashed vectors of Figure 6 represent the Hilbert-decomposed carrier wave which is used as a marker of the near-field instability driven by the free shear layer Kelvin-Helmholtz instability. The use of Hilbert transformation has been shown to effectively decompose the contribution to the velocity function, isolating the quasi-sinusoidal near-field instability u'_C with arbitrary instantaneous frequency from the downstream nonlinearity caused by rupturing of the sheet [11]. The Hilbert curves derived from u'_C follow a similar path to the raw velocity data derived from u' (solid vectors) but show less variabilty in their trajectory.

Conclusions

We have demonstrated that the temporal scaling of an annular sheet is surprisingly different from that of a planar sheet. Whereas planar sheet frequency collapses with the thickness-dependent momentum ratio and square-root thickness dependent Strouhal number, the annular sheet collapses with a geometry-independent total momentum

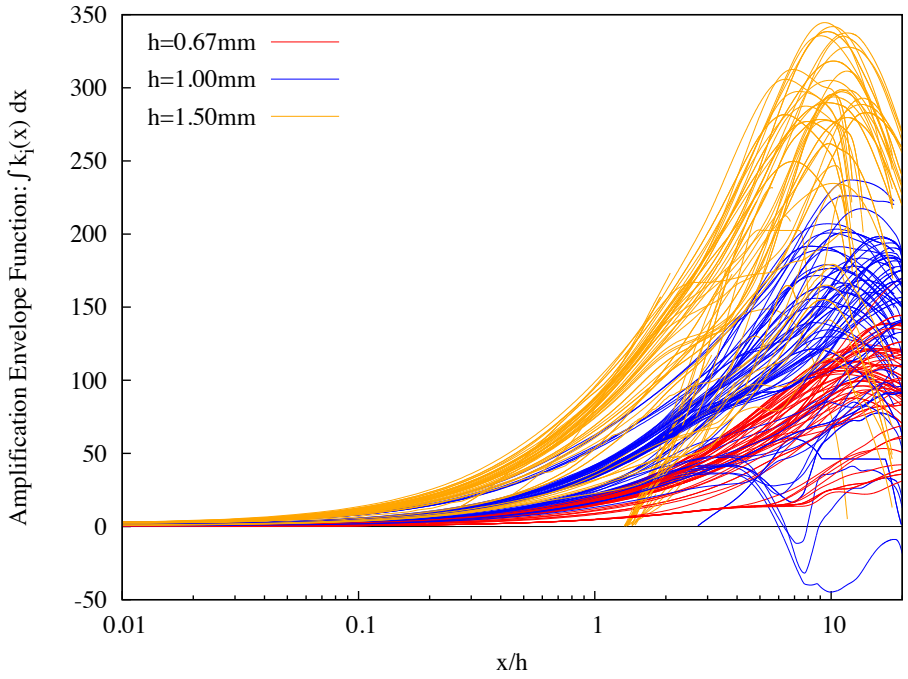

Figure 5: Non-linear amplification of instability (integral of $k_i(x)$ vs x/h) for all experiments, showing scaling behaviour of sheet thickness h. The thicker sheet exhibits a consistently larger amplification.

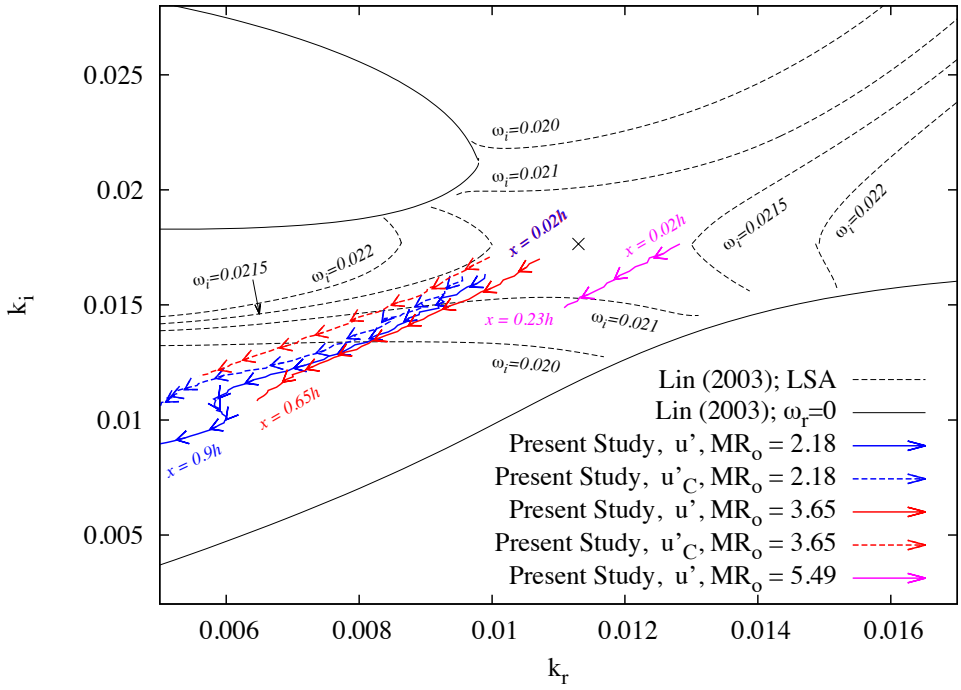

Figure 6: The plane of complex k is shown for the linear prediction of a convective instability of the sinuous type, after [1] (black lines). Comparison is given at $Re = 500, MR_i = 6 \times 10^{-3}$, with the nonlinear function $k(x)$ determined empirically via DMD for the present study at several gas-liquid momentum ratios. Coloured vectors indicate the path of the DMD eigenvalues as x/h increases for the raw velocity function (solid line) and its Hilbert-decomposed carrier wave (broken line) [11]. Near the nozzle exit, the DMD eigenvalue starts near to the saddle point of the predicted k-plane ($\times$) and rapidly shifts down and to the left, indicating an increasing wavelength and a decaying growth rate.

ratio and linear thickness-dependent Strouhal number. The question of where the transition between these scaling regimes lies as a function of sheet curvature is a matter for further study.

We have demonstrated empirically that the spatial amplification profile of the annular sheet and shows a repeatable profile and is strongly affected by a combination of non-linearity and non-parallelism. The sheet thickness has been shown to have a dominant scaling effect on the spray. A power-law relationship is proposed as the sheet thickness effect is clearly non-linear, however more sheet thicknesses need to be tested to confirm this theory.

The use of Dynamic Mode Decomposition to measure the complex wavenumber of the instability permits a direct comparison with linear stability analysis. This shows a good agreement with linear solutions of the spatially convective type. The experimental data indicates that the instability begins near the predicted point of maximum instability, but rapidly diverges from this point. The linear region in the annular spray may be smaller than the spatial resolution of the image correlation method ($\pm 21 \mu m$) and is therefore not always observed.

We wish to stress that these results are directly derived from empirical data, and that the scaling parameters (TMR, St, α, β) presented herein are yet to be supported by stability theory, unlike in the planar case. The deviation from plane sheet scaling behaviour is an interesting problem which is still to be theoretically confirmed.

Acknowledgements

The first author was supported by an Australian Postgraduate Award whilst undertaking this research, and also acknowledges the support of the Australian Fulbright Commission and the Australian Nuclear Science & Technology Organisation (ANSTO). We acknowledge the use NCI National Facility computer resources under ARC LIEF grant LE100100222.

References

[1] S Lin. *Breakup of Liquid Sheets and Jets*. Cambridge Press, 2003.

[2] A Lozano, F Barreras, Guillermo Hauke, and C Dopazo. Longitudinal instabilities in an air-blasted liquid sheet. *J. Fluid Mech.*, 437:143–173, 2001.

[3] A Lozano, F Barreras, C Siegler, and D Löw. The effects of sheet thickness on the oscillation of an air-blasted liquid sheet. *Exp. Fluids*, 39(1):127–139, 2005.

[4] S Kawano, H Hashimoto, H Togari, and A Ihara. Deformation and Breakup of An Annular Liquid Sheet in a Gas Stream. *Atom. Sprays*, 7:359–374, 1997.

[5] M Adzic, IS Carvalho, and M V Heitoyr. Visualization of the Disintegration of an Annular Liquid Sheet in a Coaxial Airblast Injector at Low Atomising Air Velocities. *Optical Diagnostics Engng*, 5(1):27–38, 2001.

[6] X Li and J Shen. Experiments on annular liquid jet breakup. *Atom. Sprays*, 11:557–573, 2001.

[7] X Li and J Shen. Experimental Study of Sprays from Annular Liquid Jet Breakup. *J. Prop. Power*, 15(1):103–110, 1999.

[8] J Kendall. Experiments on annular liquid jet instability and on the formation of liquid shells. *Phys. Fluids*, 29(7):2086–2094, 1986.

[9] P Marmottant and Emmanuel Villermaux. On spray formation. *J. Fluid Mech.*, 498:73–111, 2004.

[10] O Tammisola, A Sasaki, F Lundell, M Matsubara, and LD Söderberg. Stabilizing effect of surrounding gas flow on a plane liquid sheet. *J. Fluid Mech.*, 672:5–32, 2011.

[11] D Duke, D Honnery, and J Soria. Experimental Investigation of Nonlinear Instabilities in Annular Liquid Sheets. *J. Fluid Mech.*, 691:594–604, 2012.

[12] D Duke, D Honnery, and J Soria. A cross-correlation velocimetry technique for breakup of an annular liquid sheet. *Exp. Fluids*, 49:435–445, 2010.

[13] D Duke, D Honnery, and J Soria. A Comparison of Subpixel Edge Detection and Correlation Algorithms for the Measurement of Sprays. *Int. J. Spray Comb. Dyn.*, 3(2):93–110, 2011.

[14] D Duke, D Honnery, and J Soria. An Error Analysis of the Dynamic Mode Decomposition. *Exp. Fluids*, 52(2):529–542, 2012.

[15] S Wahono, D Honnery, J Soria, and J Ghojel. High-speed visualisation of primary break-up of an annular liquid sheet. *Exp. Fluids*, 44(3):451–459, 2008.

[16] P Schmid. Dynamic mode decomposition of numerical and experimental data. *J. Fluid Mech.*, 656:5–28, 2010.

[17] G Siamas and X Jiang. Direct numerical simulation of a liquid sheet in a compressible gas stream in axisymmetric and planar configurations. *Theor. Comput. Fluid Dyn.*, 21(6):447–471, 2007.

[18] V Sivadas, M V Heitoyr, and R Fernandes. A Functional Correlation for the Primary Breakup Processes of Liquid Sheets Emerging From Air-Assist Atomizers. *J. Fluids Eng.*, 129:188–193, 2007.

[19] A Mansour and N Chigier. Dynamic behavior of liquid sheets. *Phys. Fluids A*, 3(12):2971–2980, 1991.